Materials Science and Engineering B105 (2003) 91–96

www.elsevier.com/locate/mseb

Photoluminescence studies of rare earth (Er, Eu, Tm) in situ doped GaN

U. Hömmerich [a,*], Ei Ei Nyein [a], D.S. Lee [b], J. Heikenfeld [b], A.J. Steckl [b], J.M. Zavada [c]

[a] *Department of Physics, Hampton University, Hampton, VA 23668, USA*
[b] *Nanoelectronics Laboratory, University of Cincinnati, Cincinnati, OH 45221, USA*
[c] *US Army Research Office, Durham, NC 27709, USA*

Abstract

The emission properties of rare earth (RE)-doped GaN are of significant current interest for applications in full color displays, white lighting technology, and optical communications. We are currently investigating the photoluminescence (PL) properties of RE (Er, Eu, Tm)-doped GaN thin-films prepared by solid-source molecular beam epitaxy. The most intense visible PL under above-gap excitation is observed from GaN:Eu (red: 622 nm) followed by GaN:Er (green: 537 nm, 558 nm), and then GaN:Tm (blue: 479 nm). In this paper, we present spectroscopic results on the Ga-flux dependence of the Er^{3+} PL properties from GaN:Er and we report on the identification of different Eu^{3+} centers in GaN:Eu through high-resolution PL excitation (PLE) studies. In addition, we observed an enhancement of the blue Tm^{3+} PL from AlGaN:Tm compared to GaN:Tm. Intense blue PL from Tm^{3+} ions was also obtained from AlN:Tm under below-gap pumping.
© 2003 Elsevier B.V. All rights reserved.

PACS: 78.40. Fy; 78.55.-m; 78.55.Et

Keywords: Rare earth; GaN; AlGaN; Luminescence

1. Introduction

Rare earth (RE)-doped III-nitrides have recently emerged as a new class of phosphor materials for thin- and thick-film electroluminescence devices [1–4]. Compared to previously studied RE-doped semiconductors with relatively small band-gap (<∼1.5 eV) like e.g. GaAs or Si [5], RE doping of wide band-gap semiconductors such as GaN, AlN, and SiC has led to the observation of intense RE emission at room temperature [6,7]. In addition, studies of GaN:Er and GaN:Eu have shown that RE^{3+} ions can be incorporated into GaN at concentrations as high as 1–2 at.% without significant emission concentration quenching [8,9]. Current research efforts on RE-doped nitrides are focused on the optimization of existing materials and EL devices [2,3,7], evaluation of different doping techniques and dopant/host combinations [4,7,10–12], as well as fundamental spectroscopic studies aimed towards a better understanding of the RE incorporation, excitation schemes, and emission efficiency [7,13–16].

In this paper, we present spectroscopic results of the PL properties of GaN:Er as a function of Ga-flux employed during molecular beam epitaxy (MBE) growth. As will be discussed in more detail, the Ga-flux during growth significantly impacts the Er^{3+} lattice location and the concentration of optically active Er^{3+} ions. High-resolution PL excitation (PLE) studies were carried out on GaN:Eu, which allowed the identification of $^5D_0 \leftrightarrow {}^7F_0$ transitions and associated Eu^{3+} centers. Finally, we report on initial PL studies of Tm-doped $Al_xGa_{1-x}N$ ($0 \leq x \leq 1$) and the enhancement of the blue Tm^{3+} emission with increasing Al content.

2. Experimental details

Rare earth (Er, Eu, Tm)-doped GaN and Tm-doped $Al_xGa_{1-x}N$ films with $x = 0.13$, 0.24, 0.29, 0.44, and 1 (AlN) were grown by solid-source MBE on p-type Si(1 1 1) substrates. Elemental Ga, Al, and RE sources were used in conjunction with a radio frequency (rf)-plasma source supplying atomic nitrogen. The RE concentration in the GaN and AlGaN films varied between ∼0.5 and ∼1 at.%. More details on the sample preparation were published previously [2,17].

* Corresponding author. Tel.: +1-757-727-5829; fax: +1-757-728-6910.
E-mail address: uwe.hommerich@hamptonu.edu (U. Hömmerich).

0921-5107/$ – see front matter © 2003 Elsevier B.V. All rights reserved.
doi:10.1016/j.mseb.2003.08.022

PL spectra were measured using either the UV argon laser lines (336–363 nm) or a visible argon laser line at 496.5 nm. PL excitation spectra were recorded using an Optical Parametric Oscillator system as the excitation source. For low-temperature PL measurements the samples were mounted on the cold-finger of a closed-cycle helium refrigerator. Infrared PL spectra were recorded using a 1 m monochromator equipped with a liquid-nitrogen cooled Ge detector. In visible PL studies a thermo-electric cooled photomultiplier tube was employed for detection. The signal was processed using lock-in techniques or using a boxcar averager. The obtained PL spectra were not corrected for the spectral response of the setup.

3. Results and discussion

3.1. Er-doped GaN

It was previously reported that the visible and infrared emission properties of Er^{3+} ions in GaN films are strongly dependent on the Ga-flux during growth [18]. Under above band-gap excitation the Er^{3+} PL emission reached its maximum under slightly N-rich growth conditions. On the contrary, the band-edge emission from the GaN host reached its maximum under Ga-rich growth. This observation lead to the conclusion that the Ga-flux strongly influences the carrier-mediated excitation efficiency of Er^{3+} ions [18]. In the following, more detailed spectroscopic study on the Ga-flux dependence of the Er^{3+} PL properties are presented. Er-doped GaN samples grown under Ga-fluxes with beam equivalent pressures ranging from 2.2×10^{-7} Torr ("N-rich") to 6.9×10^{-7} Torr ("Ga-rich") were investigated [18]. The stoichiometric growth condition as determined by film thickness saturation was ~4 to 5×10^{-7} Torr.

The visible and IR PL spectra under below band-gap excitation (496.5 nm) are shown in Fig. 1. This excitation wavelength overlaps an intra-4f Er^{3+} absorption line ($^4I_{15/2} \rightarrow {}^4F_{9/2}$) [19,20]. Similar to above-gap excitation [18], the Er^{3+} PL strongly varied with Ga-flux under resonant excitation and reached a maximum under slightly N-rich growth condition. Since both excitation schemes, carried-mediated and resonant intra-4f, exhibited the same Er^{3+} PL behavior it can be concluded that the carrier-mediated Er^{3+} excitation is only weakly affected by the Ga-flux during growth.

Fig. 2 shows the high-resolution 1.54 μm Er^{3+} PL spectra of GaN:Er samples grown under different Ga-fluxes. A significant decrease in the 1.54 μm PL linewidth can be noticed as well as the appearance of new spectral features with increasing Ga-flux. The spectral narrowing of the emission lines is consistent with the higher crystalline quality of GaN grown under Ga-rich conditions [18,21]. The observation of new spectral lines indicates that Er^{3+} ions are incorporated into different lattice locations depending on the Ga-flux.

More information on the optical activation of Er^{3+} in GaN can be drawn from power dependent PL studies under above-gap excitation (see Fig. 3). All investigated samples exhibited the onset of 1.54 μm PL saturation at relatively low pump intensities (<2 W/cm^2), consistent with a high excitation efficiency for above-gap pumping [16]. At the same time, it can be noticed that the Er^{3+} PL saturation level greatly varied for the different samples. It has been discussed in the literature before [16,22], that the Er^{3+} PL saturation level is determined by the product of concentration of optically active Er ions (N_{Er}) and radiative decay rate (w_{rad}). PL lifetime studies revealed that w_{rad} is approximately independent of Ga-flux. Therefore, the large difference in the PL saturation is attributed to a large difference in the concentration of optically active Er^{3+} ions. As can be derived from Fig. 3, the PL saturation level and hence N_{Er} is ~17 times larger for the sample grown under slightly N-rich con-

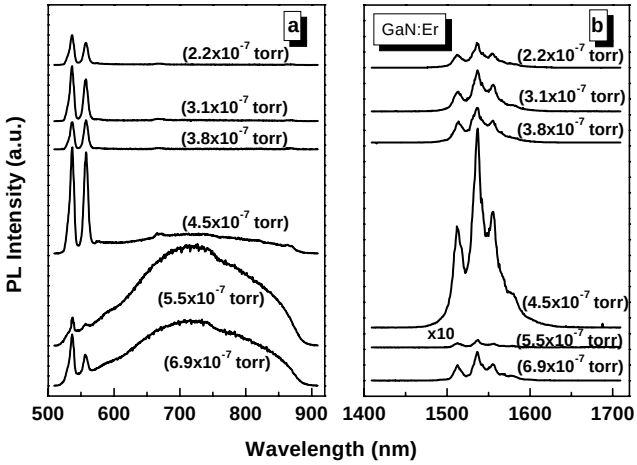

Fig. 1. Visible (a) and infrared (b) emission from Er-doped GaN as a function of Ga-flux under below-gap excitation (496.5 nm). For both cases, the Er^{3+} emission intensity reached its maximum under slightly N-rich flux near the stoichiometric growth condition (Ga-flux: $\sim 4.5 \times 10^{-7}$ Torr).

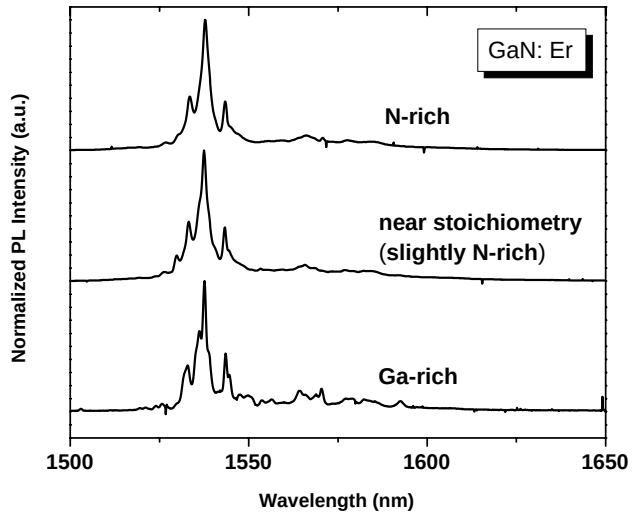

Fig. 2. High-resolution, infrared emission spectra at 15 K from Er-doped GaN grown under different Ga-fluxes. The emission was excited using below-gap excitation (496.5 nm).

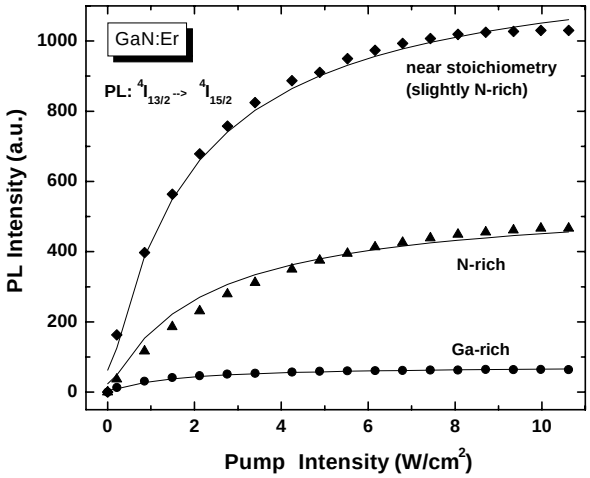

Fig. 3. Pump intensity dependence of the 1.54 μm PL from GaN:Er samples grown with different Ga-flux during growth. The emission was excited using above-gap excitation (336–363 nm). The solid lines are guides for the eye.

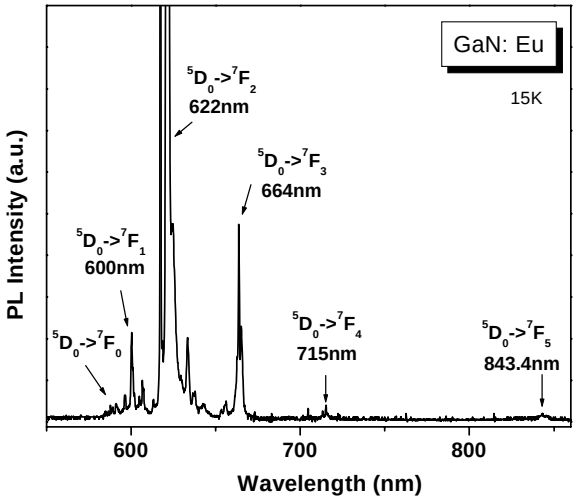

Fig. 4. Emission spectrum of GaN:Eu at 15 K under above-gap excitation. The main emission features arising from the $^5D_0$–^7F_J (J = 0,1,2,3,4,5) transitions are indicated in the graph. More details on the identification of the $^5D_0$–$^7F_0$ transitions are presented in Fig. 5.

ditions compared to that grown under Ga-rich conditions. In contrast, previous secondary ion mass spectroscopy (SIMS) studies have shown that the total Er concentration in the investigated GaN:Er films varied only by roughly a factor of two [18]. Therefore, the PL saturation result from Fig. 3 reveal that in GaN:Er grown under Ga-rich conditions only a small fraction (<10%) of the total Er concentration is optically active under above-gap pumping. Similar observations were reported for Er-doped crystalline and amorphous Si [23]. More comparative PL saturation studies employing a well-characterized Er^{3+} sample (e.g. Er-doped SiO_2) are required to determine the absolute concentration of optically active Er^{3+} ions in GaN:Er.

3.2. Eu-doped GaN

Eu-doped GaN is of great interest for display applications because of its bright red emission peaking around 622 nm [14,24–28]. Eu^{3+} is also known as a "spectroscopic probe" for the local environment of Eu^{3+} ions in solids, because the main emitting level is the non-degenerate $^5D_0$ state [20]. For example, observing the $^5D_0 \leftrightarrow {}^7F_0$ transition allows one to identify the number of emitting Eu^{3+} centers in a given host. Fig. 4 gives an overview of the low temperature emission of GaN:Eu. The main emission lines can be assigned to the transitions: $^5D_0 \rightarrow {}^7F_5$ (∼843 nm), $^5D_0 \rightarrow {}^7F_4$ (∼715 nm), $^5D_0 \rightarrow {}^7F_3$ (∼664 nm), $^5D_0 \rightarrow {}^7F_2$ (∼622 nm), and $^5D_0 \rightarrow {}^7F_1$ (∼600 nm). The weak emission features at ∼585 and ∼590 nm are most likely due to $^5D_0 \rightarrow {}^7F_0$ transitions suggesting multiple Eu^{3+} centers in GaN [14,27,28].

In order to identify the $^5D_0 \leftrightarrow {}^7F_0$ transitions and associated Eu^{3+} centers more clearly, we have performed high-resolution PL excitation studies in the range from 560 to 595 nm. The spectral resolution in the PLE measurements was limited by the linewidth of the employed excitation source (∼0.2 cm^{-1}) (Fig. 5).

At room temperature, four PLE peaks were observed at 571, 585.2, 588.8, and 591.7 nm. With decreasing temperature the peak at 591.7 nm reduced in intensity and was not observed at 15 K. Therefore, this line does not originate from the $^7F_0$ ground state, but is due to the thermal population of higher lying $^7F_1/{}^7F_2$ manifolds. The linewidth of all PLE peaks observed at room-temperature narrowed slightly with decreasing temperature and some fine structure was resolved. At low temperature (15 K) five PLE lines at 571, 585.8, 587.9, 588.9, and 589.4 nm were observed and tentatively assigned to $^7F_0 \rightarrow {}^5D_0$ transitions. The $^7F_0 \rightarrow {}^5D_0$ transition at ∼571 nm is at an unusually low wavelength, but similar cases have been reported [29,30]. Therefore, we conclude that at least five different Eu^{3+} centers exist in GaN:Eu.

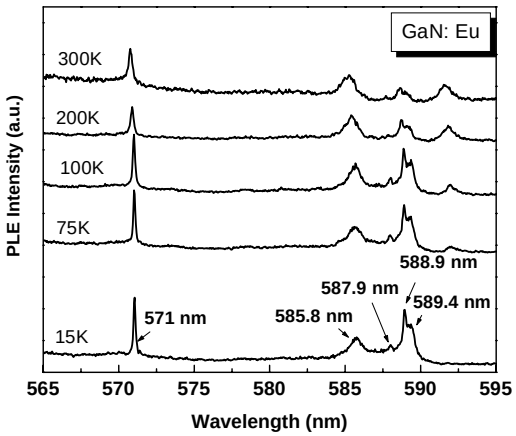

Fig. 5. High-resolution PLE spectrum of Eu-doped GaN at 15 K. The emission was monitored at ∼623 nm. Absorption lines located at 571, 585.5, 587.9, 588.9, and 589.4 nm are tentatively assigned to the $^7F_0$–$^5D_0$ transitions.

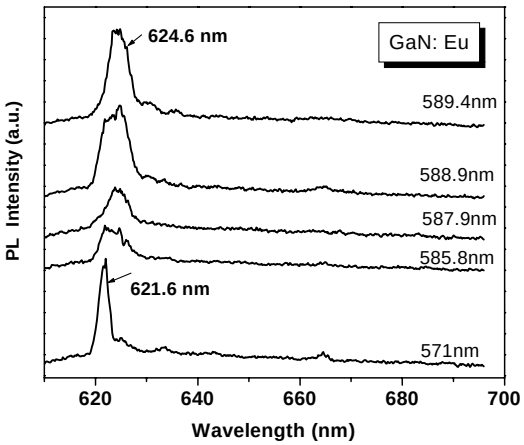

Fig. 6. Site-selective PL spectra at 15 K excited at 571, 585.5, 587.9, 588.9, and 589.4 nm. The Eu^{3+} center excited at 571 nm is distinct from the other Eu^{3+} centers and dominates under above-gap excitation.

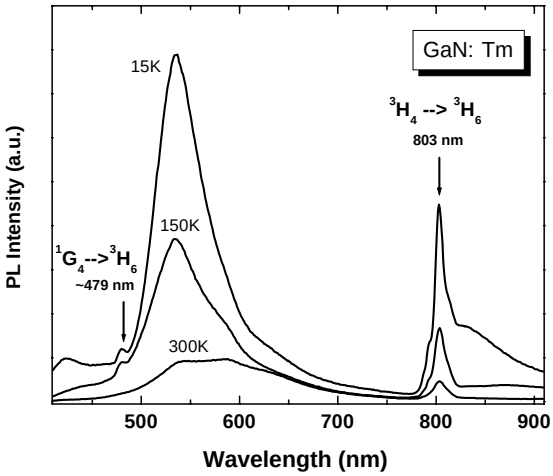

Fig. 7. PL spectra of Tm-doped GaN under above-gap excitation at 15, 150, and 300 K. The shoulder at 479 nm indicates blue emission from the $^1G_4 \rightarrow {}^3H_6$ intra-4f transition of Tm^{3+}.

More support for the identification of the different Eu^{3+} centers was obtained from site-selective PL measurements. Pumping resonantly into each of the PLE line revealed different Eu^{3+} emission spectra and lifetimes as shown in Fig. 6. The spectral differences are especially pronounced for the Eu^{3+} center excited at 571 nm. This Eu^{3+} center exhibited a relatively narrow $^5D_0 \rightarrow {}^7F_2$ PL at ~622 nm with a nearly exponential lifetime of ~235 μs. The $^5D_0 \rightarrow {}^7F_2$ PL spectra of the other Eu^{3+} centers are broader and shifted to longer wavelength (~624 nm). In addition, the PL decay transients of these Eu^{3+} centers are non-exponential with average lifetimes of less than 200 μs. The smaller linewidth of the 571 nm Eu^{3+} center indicates less inhomogeneous broadening compared to the other Eu^{3+} centers. It can be speculated that the 571 nm center is associated with Eu^{3+} ions in substitutional Ga^{3+} lattice positions, whereas the other Eu^{3+} centers are due to Eu^{3+} ions incorporated into interstitial sites with close vicinity to other defects and impurities. Interestingly, the PL spectrum excited at 571 nm is very similar to PL spectra obtained under above-gap pumping, which shows that this Eu^{3+} center dominates under carrier-mediated excitation. More site-selective PL and PLE studies of the different Eu^{3+} centers in GaN are in progress.

3.3. *Tm-doped $Al_xGa_{1-x}N$ ($0 \leq x \leq 1$)*

PL spectra of Tm-doped GaN under above-gap excitation at 15, 150, and 300 K are shown in Fig. 7. The emission is dominated by a broad band centered at ~530 nm, which extends from roughly 450 to 750 nm and resembles the well-known yellow band emission from GaN [31,32]. An infrared emission line at ~803 nm can be assigned to the intra-4f transition $^3H_4 \rightarrow {}^3H_6$ of Tm^{3+} ions [33]. A weak shoulder at ~479 nm indicates the blue emission line from the $^1G_4 \rightarrow {}^3H_6$ transition of Tm^{3+}. The PL intensity of 479 nm line increases slightly when cooling the sample down to 15 K. Compared to the visible PL from GaN:Er and GaN:Eu, the blue emission from GaN:Tm is orders of magnitude weaker under above-gap pumping, which indicates that Tm^{3+} ions are not efficiently excited through carrier recombination processes.

An energy transfer model based on a RE-related trap level was proposed by Takahei et al. for InP:Yb and later extended to other RE-doped semiconductors [34,35]. In this model, RE doping of a semiconductor leads to the formation of a RE related level in the band-gap of the host. This level can trap photo-excited free carriers, which subsequently recombine and transfer their energy to intra-4f RE transitions. Our recent PL excitation measurements of GaN:Eu provided experimental evidence for an Eu trap-level at ~0.3 eV below the conduction band of GaN [27]. A similar level was reported by Li et al. using Fourier transform infrared (FTIR) measurements [9] and by Vantomme et al. using deep level transient spectroscopy (DLTS) [36]. An Er related trap-level at ~0.3 eV was also reported for GaN:Er [37]. The recombination energy of carriers trapped at the Eu/Er related traps in GaN is then estimated to be ~3.1 eV, which energetically matches intra-4f transitions of Eu^{3+} and Er^{3+}, respectively [19]. Therefore, the carrier-mediated energy transfer to Er^{3+} and Eu^{3+} seems to occur with high efficiency. On the contrary, the energy level structure of Tm^{3+} does not exhibit an energy level at ~3.1 eV. Consequently, a carrier-mediated energy transfer process to Tm^{3+} ions is less likely to occur in GaN:Tm. A similar explanation was recently proposed for the poor above-gap excitation efficiency of Tb^{3+} ions in GaN:Tb [9].

In an effort to optimize the carrier-mediated excitation of Tm^{3+} ions in III-nitrides, we are currently exploring the energy transfer process to Tm^{3+} as a function of band-gap energy. Fig. 8 shows preliminary emission spectra for Tm-doped $Al_xGa_{1-x}N$ with $x = 0$ (GaN), 0.13,0.24, 0.29, 0.44, and 1 (AlN). The corresponding band-gap energies are 3.4 eV (GaN), 3.64, 3.88, 3.99, 4.89, and 6.2 eV (AlN)

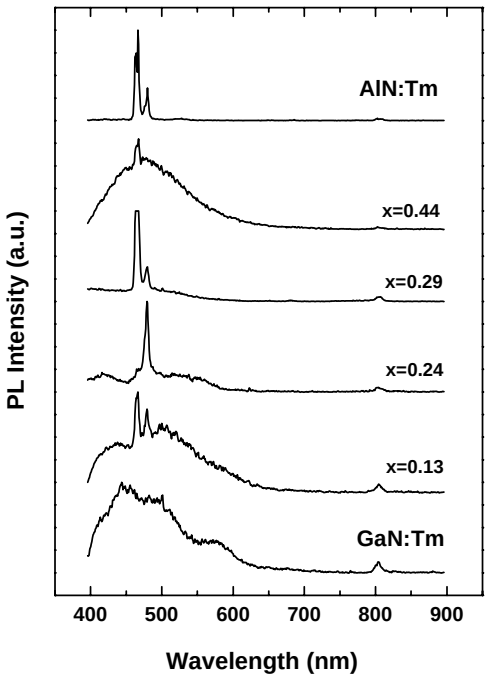

Fig. 8. PL spectra of Tm-doped $Al_xGa_{1-x}N$ with $x = 0$ (GaN), 0.13, 0.24, 0.29, 0.44, and 1 (AlN) under 250 nm excitation.

respectively. The emission was excited at 250 nm, which corresponds to above-gap pumping for all investigated AlGaN samples, but results in below-gap excitation for AlN:Tm. As discussed before, hardly any blue emission was observed from GaN:Tm (lowest trace in Fig. 8). With increasing Al content an enhancement of the 478 nm line from Tm^{3+} is observed. In addition, a new blue emission line appears at ~466 nm. Based on a comparison to existing literature [38], the 466 nm line is tentatively attributed to emission from the $^1D_2 \rightarrow {}^3F_4$ transition of Tm^{3+} ions. The overall blue emission from both lines at 466 and 479 nm reached a maximum for an Al content of $x = 0.29$, with the 466 nm line having the highest PL intensity. At higher Al content the total blue emission started to decrease and at $x = 0.44$ only weak blue emission at 466 nm was observed. On the contrary, below-gap pumping at 250 nm of AlN:Tm resulted into strong blue emission with intense lines at ~466 and 479 nm. For AlN:Tm, the blue emission is most likely excited through some broad defect level in the host.

Fig. 8 clearly demonstrates the sensitivity of the blue Tm^{3+} emission on the Al content and hence the band-gap of AlGaN. It cannot be excluded, however, that also chemical effects related to the presence of Al change the Tm^{3+} incorporation and excitation mechanisms, similar to observations made for Er-doped AlGaAs [39,40]. The initial spectroscopic data on $Al_xGa_{1-x}N$:Tm indicate that the excitation efficiency of the $^1G_4$ state of Tm^{3+} increases up to $x \sim 0.24$. In addition, the larger bandgap of AlGaN compared to GaN moves the $^1D_2$ level of Tm^{3+} within the band-gap of the host, which results in emission at 466 nm. A more detailed analysis of the emission properties of AlGaN:Tm and AlN:Tm is still in progress and will be discussed in a forthcoming paper.

4. Conclusions

Spectroscopic results on the PL properties of GaN:Er, GaN:Eu, GaN:Tm and AlGaN:Tm were presented. High-resolution PL and pump-power dependent PL studies of GaN:Er samples revealed that the Er^{3+} incorporation and the concentration of optically active Er ions is strongly dependent on the Ga-flux during MBE growth. Based on PL saturation experiments, we concluded that only a small fraction (<10%) of the total Er ions in GaN are optically active for samples grown under Ga-rich conditions. More PL saturation experiments are still in progress to determine the absolute concentration of optically active Er^{3+} ions in GaN:Er films. The low optical activation of Er^{3+} ions in GaN is similar to recent observations made for Er-doped Si/amorphous Si [23]. This issue needs to be further addressed in future investigations to explore the full potential of RE-doped GaN for device applications. High-resolution PL excitation studies were performed on GaN:Eu and allowed the identification of at least five Eu^{3+} centers. An absorption line at an unusually low wavelength of ~571 nm was also tentatively assigned to the $^5D_0 \leftrightarrow {}^7F_0$ transition. The Eu^{3+} center selectively excited through this 571 nm absorption line is distinct from the other Eu^{3+} centers and seems to dominate the above-gap pumped PL emission spectrum. GaN:Tm exhibited only a weak blue emission from the $^1G_4 \rightarrow {}^3H_6$ transition of Tm^{3+} ions. A significant enhancement of the blue Tm^{3+} emission was obtained under above-gap pumping of Tm-doped $Al_xGa_{1-x}N$ samples. Besides emission from the $^1G_4 \rightarrow {}^3H_6$ transition, a second blue emission line appeared around 466 nm for $x > 0.13$, which was assigned to the $^1D_2 \rightarrow {}^3F_4$ transition of Tm^{3+}. Strong blue emission from the $^1D_2$ and $^1G_4$ levels of Tm^{3+} was also observed from Tm-doped AlN under below-gap excitation. The large sensitivity of the blue emission from Tm^{3+} on the band-gap of AlGaN suggests the possibility to optimize the RE excitation and emission properties through careful band-gap engineering of the host.

Acknowledgements

The authors from H.U. acknowledge financial support by ARO through grant DAAD19-02-1-0316. The work at U.C. was supported by ARO grant DAAD19-99-1-0348. Helpful discussions with F. Pelle and F. Auzel are also acknowledged.

References

[1] A.J. Steckl, J.M. Zavada, MRS Bull. 24 (9) (1999) 33–38.
[2] A.J. Steckl, J.C. Heikenfeld, D.S. Lee, M.J. Garter, C.C. Baker, Y. Wang, R. Jones, IEEE J. Sel. Top. Quant. 8 (2002) 749.

[3] S. Morishima, T. Maruyama, M. Tanaka, Y. Masumoto, K. Akimoto, Phys. Stat. Sol. A 176 (1999) 113.
[4] V.I. Dimitrova, P.G. Van Patten, H.H. Richardson, M.E. Kordesh, Appl. Phys. Lett. 77 (2000) 478.
[5] Rare earth doped semiconductors. I, in: G.S. Pomerenke, P.B. Klein, D.W. Langer (Eds.), Proceedings of the Materials Research Society, Vol. 301, 1993.
[6] Rare earth doped semiconductors. II, in: S. Coffa, A. Polman, R.N. Schwartz, (Eds.), Proceedings of the Materials Research Society, Vol. 422, 1996.
[7] Rare earth doped semiconductors. III, in: J. Zavada, T. Gregorkiewicz, A.J. Steckl (Eds.), Proceedings of E-MRS Symposium Spring 2000, Mater. Sci. Eng. B 81 (2001).
[8] D.S. Lee, J. Heikenfeld, A.J. Steckl, U. Hömmerich, J.T. Seo, A. Braud, J.M. Zavada, Appl. Phys. Lett. 79 (2001) 719.
[9] Z. Li, H. Bang, G. Piao, J. Sawahata, K. Akimoto, J. Cryst. Growth 240 (2002) 382.
[10] J.T. Torvik, C.H. Qui, R.J. Feuerstein, J.I. Pankove, F. Namavar, J. Appl. Phys. 81 (1997) 6343.
[11] H.J. Lozykowski, W.M. Jadwisienczak, I.G. Brown, Appl. Phys. Lett. 74 (1999) 1129.
[12] E. Alves, M.F. da Silva, J.C. Soares, R. Vianden, J. Bartels, A. Kozanecki, Nucl. Instrum. Methods B 147 (1999) 383.
[13] S. Kim, S.J. Rhee, X. Li, J.J. Coleman, S.G. Bishop, P.B. Klein, J. Electron. Mater. 27 (1998) 246.
[14] T. Monteiro, C. Boemare, M.J. Soares, R.A. Sa Ferreira, L.D. Carlos, K. Lorenz, R. Vianden, E. Alves, Physica B 308–310 (2001) 22.
[15] U. Wahl, A. Vantomme, G. Langouche, J.P. Araujo, L. Peralta, J.G. Correia,. The ISOLDE collaboration J. Appl. Phys. 88 (2000) 1319.
[16] J.T. Seo, U. Hömmerich, D.S. Lee, J. Heikenfeld, A.J. Steckl, J.M. Zavada, J. Alloys Comp. 342 (2002) 62.
[17] A. Steckl, R. Birkhahn, Appl. Phys. Lett. 73 (1998) 1700.
[18] D.S. Lee, A.J. Steckl, Appl. Phys. Lett. 80 (2002) 728.
[19] G.H. Dieke, Spectra and Energy Levels of Rare Earth Ions in Crystals, Wiley, New York, 1968.
[20] B. Henderson, G.F. Imbusch, Optical Spectroscopy of Inorganic Solids, Clarendon Press, Oxford, UK, 1989.
[21] E. Calleja, M.A. Sanchez-Garcia, F.J. Sanchez, F. Calle, F.B. Naranjo, E. Munoz, U. Jahn, K. Ploog, Phys. Rev. B 62 (2000) 16826.
[22] F. Priolo, G. Franzo, S. Coffa, A. Carnera, Phys. Rev. B. 57 (1998) 4443.
[23] O.B. Gusev, M.S. Bresler, P.E. Pak, I.N. Yassievich, M. Forcales, N.Q. Vinh, T. Gregorkiewicz, Phys. Rev. B 64 (2001) 075302.
[24] J. Heikenfeld, M. Garter, D.S. Lee, R. Birkhahn, A.J. Steckl, Appl. Phys. Lett. 75 (1999) 1189.
[25] H.J. Lozykowski, W.M. Jadwisienczak, J. Han, I.G. Brown, Appl. Phys. Lett. 77 (2000) 767.
[26] M. Overberg, K.N. Lee, C.R. Abernathy, S.J. Pearton, W.S. Hobson, R.G. Wilson, J.M. Zavada, Mater. Sci. Eng. B 81 (2001) 150.
[27] E.E. Nyein, U. Hommerich, J. Heikenfeld, D.S. Lee, A.J. Steckl, J.M. Zavada, Appl. Phys. Lett. 82 (2003) 1655.
[28] H. Bang, S. Morishima, Z. Li, K. Akimoto, M. Nomura, E. Yagi, Phys. Stat. Sol. B 228 (2001) 319.
[29] R. Ternane, G. Panczer, M.Th. Cohen-Adad, C. Goutaudier, G. Boulon, N. Kbir-Ariguib, M. Trabesli-Ayedi, Opt. Mater. 16 (2001) 291.
[30] E. Antic-Fidancev, J. Alloys Comp. 300301 (2002) 2.
[31] T. Ogino, M. Aoki, Jpn. J. Appl. Phys. 19 (1980) 2395.
[32] S.J. Pearton, J.C. Zolper, R.J. Shul, F. Ren, J. Appl. Phys. 86 (1999) 1.
[33] D.S. Lee, A.J. Steckl, Appl. Phys. Lett. 82 (2003) 55.
[34] K. Takahei, A. Taguchi, H. Nakagome, K. Uwai, P.S. Whitney, J. Appl. Phys. 66 (1989) 4941.
[35] A. Taguchi, K. Takahei, J. Appl. Phys. 79 (1996) 4330.
[36] A. Vantomme, B. Pipeleers, V. Matias, E. Alves, K. Lorenz, R.W. Martin, S. Dalmasso, K.P. O'Donnell, A. Braud, J.L. Doualan, European Materials Society Spring Meeting 2003, Strasbourg, France, paper J-VI.1.
[37] S. Kim, S.J. Rhee, X. Li, J.J. Coleman, S.G. Bishop, P.B. Klein, J. Electron. Mater. 27 (1998) 246.
[38] J.B. Gruber, A.O. Wright, M.D. Selter, B. Zandi, L.D. Merkle, J.A. Hutchinson, C.A. Morrison, T.H. Allik, B.H.T. Chai, J. Appl. Phys. 81 (1997) 6585.
[39] T. Zhang, J. Sun, N.V. Edwards, D.E. Moxey, R.M. Kolbas, P.J. Caldwell, Mater. Res. Soc. Symp. Proc. 301 (1993) 257.
[40] T.D. Culp, U. Hömmerich, J.M. Redwing, T.F. Kuech, K.L. Bray, J. Appl. Phys. 82 (1997) 368.